ELSEVIER

Int. J. Therm. Sci. 41 (2002) 639–645

International Journal of Thermal Sciences

www.elsevier.com/locate/ijts

Condensation heat transfer of herringbone micro fin tubes ☆

Akio Miyara [a,*], Yusuke Otsubo [b]

[a] *Department of Mechanical Engineering, Saga University 1 Honjomachi, Saga-shi 840-8502, Japan*
[b] *Graduate School of Science and Engineering, Saga University 1 Honjomachi, Saga-shi 840-8502, Japan*

Received 29 October 2001; accepted 8 February 2002

Abstract

Experiments of in-tube condensation of R410A were carried out for a smooth tube, a helical micro fin tube and three types of herringbone micro fin tubes, which have different fin height and helix angle. In the herringbone micro fin tube, the micro fins work to remove liquid at fin-diverging parts and collect liquid at fin-converging parts. In the high mass velocity region the heat transfer coefficients of all the herringbone tubes are higher than those of the helical micro fin tube. In the low mass velocity region, however, the heat transfer coefficients of the herringbone micro fin tubes are slightly lower than those of the helical micro fin tube. The heat transfer coefficient is lower for smaller helix angle tube and effect of fin height on the heat transfer is small. Pressure drop of the herringbone tube of which helix angle is small is lower than that of the helical micro fin tube, while that of other tubes is higher. Flow configurations of the herringbone tubes were observed with R123 as working fluid and the heat transfer enhancement mechanism is discussed.

Keywords: Condensation; Herringbone micro fin tube; Heat transfer; Pressure drop; Heat transfer enhancement; Flow configuration

1. Introduction

From the end of 1970s, condensation and evaporation heat transfer inside a horizontal tube in heat exchangers of refrigeration systems and air conditioners is enhanced by micro fin tubes, in which helical micro fins are installed inside of the tube. It is known that the heat transfer coefficient of the helical micro fin tubes is about two times that of the smooth tube, while the pressure drop is not so high. Up to the middle of 1990s, the micro fin tube has been improved by changing the fin and groove shapes from triangular to trapezoidal and by enlarging the fin height from $0.15 \sim 0.18$ mm to $0.18 \sim 0.25$ mm. The enhancement rate becomes about $2.5 \sim 3.0$. Recently, herringbone micro fin tubes reported by Okazaki et al. [1], Ebisu et al. [2] and Miyara et al. [3] and cross-grooved micro fin tubes reported by Chamra et al. [4] and Uchida et al. [5] are produced as new advanced tubes. For both types of the tubes, it has been reported that the heat transfer coefficient is much higher than that of the conventional helical micro fin tubes. The herringbone micro fin tube, in which herringbone micro fins are installed, is addressed in the present study. Because of limited experimental data, the heat transfer enhancement mechanism is not sufficiently explained and effects of fin shape, fin direction, mass velocity, and fluid properties are not clarified.

In this paper, the heat transfer coefficient and pressure drop during the condensation of R410A inside a smooth tube, a helical micro fin tube, and three types of herringbone micro fin tubes are measured. Effects of fin height, helix angle, and mass velocity are especially discussed. Flow configurations at the tube outlet of the herringbone micro fin tube are observed by using R123 as a working fluid. The heat transfer enhancement mechanism of the herringbone micro fin tube is also discussed.

2. Experimental method

The experimental apparatus is a vapor compression heat pump loop composed of a compressor, an oil separator, a test condenser, a subcooler, an expansion valve and an evaporator. Cooling water kept at a constant temperature is

☆ This article is a follow-up a communication presented by the authors at the ExHFT-5 (5th World Conference on Experimental Heat Transfer, Fluid Mechanics and Thermodynamics), held in Thessaloniki in September 24–28, 2001.

* Correspondence and reprints.
E-mail address: miyara@me.saga-u.ac.jp (A. Miyara).

1290-0729/02/$ – see front matter
PII: S1290-0729(02)01358-3

Nomenclature

b	fin space	m
d_i	inner diameter, or average inner diameter	m
d_o	outer diameter	m
G	mass velocity	$kg{\cdot}m^{-2}{\cdot}s^{-1}$
k	tube thickness	m
l	fin height	m
p	fin pitch	m
P	pressure	Pa
q	heat flux	$W{\cdot}m^{-2}$
Q	heat transfer rate	W
t	fin tip thickness	m
T	temperature	°C or K
x	thermodynamic quality	
z	axial distance	m
Δz	length of subsection	m

Greek symbols

α	heat transfer coefficient, Eq. (1)	$W{\cdot}m^{-2}{\cdot}K^{-1}$
α	apex angle	
β	helix angle	
λ	dimensionless parameter, Eq. (5)	
λ_w	thermal conductivity of test tube	$J{\cdot}m^{-1}{\cdot}s^{-1}{\cdot}K^{-1}$
μ	dynamic viscosity	Pa·s
ρ	density	$kg{\cdot}m^{-3}$
ψ	dimensionless parameter, Eq. (6)	

Subscripts

0	inlet of test condenser
A	air at 1 atm and 20 °C
L	liquid
s	saturation
V	vapor
wi	inner wall surface of test tube
wo	outer wall surface of test tube
W	water at 1 atm and 20 °C

supplied to the test condenser from a cooling water unit. The flow rate of the refrigerant is regulated by varying the rotating speed of the compressor and opening the expansion valve and it is measured by a mass flow meter. Although the concentration of refrigeration oil has not been measured experimentally, it is estimated to be about 0.1% at the oil separator outlet. Therefore, the influence of the oil is ignored.

Fig. 1(a) shows an outline of the test section. The test section is a horizontally installed double tube heat exchanger with a length of 4 meters. Refrigerant flows inside an inner tube and cooling water flows through the annular space in counter current. In order to measure quasi-local heat transfer, the annular channel is divided into 12 subsections. Effective heat transfer length of the subsection is 300 mm. The inner tube is a test tube made of copper of 7.0 mm outer diameter. Inner diameter of the outer tube is 11.1 mm.

Temperature of cooling water is measured at inlet/outlet of each subsection. At the central positions of each subsection the circumferential temperature distribution of the outer surface of the inner test tube is measured with copper-constantan thermocouples. As shown in Fig. 1(b), the four constantan wires with a diameter of 0.1 mm are welded on the top, bottom, right and left sides of the test tube, and a copper wire with a diameter of 0.1 mm is welded 25 mm away from the central position. The temperatures are measured at constantan-tube junctions and an effect of a tube-copper junction is very small, because a difference of the materials is small. The electromotive force at the tube-copper junction is about 4.5×10^{-5} $mV{\cdot}K^{-1}$, which affects on a measurement only about 0.01 K per 1 K-temperature difference between junctions of constantan-tube and tub-copper. Refrigerant temperature and pressure in the test tube are measured at every 1 m length. Small amount of refrigerant is sampled after the subcooler and its concentration is measured by a gas chromatograph. During a series of the experiments of R410A, of which nominal concentration is R32/R125 of 50/50 mass %, the concentration was slightly different from the nominal concentration and that of R32 changed fractionally from 48.0 to 51.9 mass %. The measured concentrations were used to estimate the thermodynamic and transport properties although the variations were small. All the thermocouples were calibrated within an error of ± 0.05 K. An absolute pressure transducer and a differential pressure transducer were calibrated within errors of ± 0.5 kPa and ± 0.05 kPa, respectively. Flow rates of the refrigerant and cooling water were measured with a mass flow meter and a magnetic flow meter, respectively, in which they were calibrated within errors of $\pm 6.0 \times 10^{-5}$ $kg{\cdot}s^{-1}$ and $\pm 2.5 \times 10^{-4}$ $kg{\cdot}s^{-1}$.

Refrigerant enters the test section as a superheated vapor with superheat of $5 \sim 7$ K and leave it as a subcooled liquid with subcool of $10 \sim 12$ K. Because the degree of the superheat is small, there is a little effect on the heat transfer coefficient. Enthalpy changes of the refrigerant and the cooling water are compared and an error of the heat balance is within $\pm 10\%$.

Configurations of the helical micro-fin tube and the herringbone micro fin tube are illustrated in Fig. 2 and dimensions of each tube are shown in Table 1. In the present study a smooth tube S-1, a helical micro fin tube G-1, and three types of herringbone micro fin tubes H-1 $\sim$ 3 are tested.

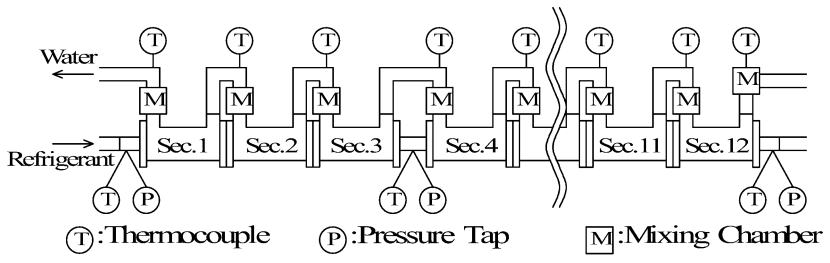

(a) Outline of test section

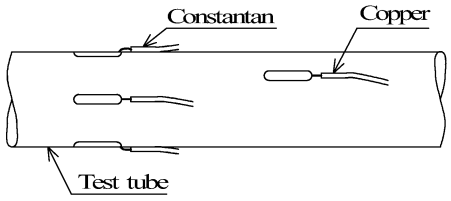

(b) Thermocouple installation

Fig. 1. Test section: (a) Outline of test section; (b) Thermocouple installation.

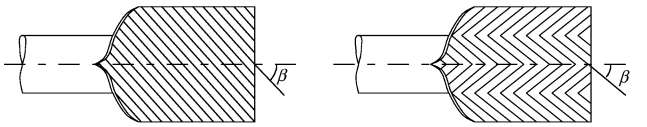

(a) helical micro fin tube (b) herringbone micro fin tube

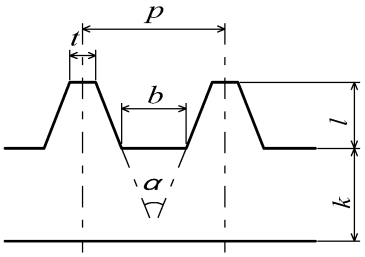

(c) cross section of fin

Fig. 2. Configurations of test tubes: (a) Helical micro fin tube; (b) Herringbone micro fin tube; (c) Cross-section of fin.

In the herringbone micro fin tube, micro fins work to remove liquid at fin-diverging parts and collect liquid at fin-converging parts. The heat transfer is enhanced by making thinner film at the diverging parts and by mixing the liquid at the converging parts. When the tube is arranged as the diverging parts are both sides and converging parts are top and bottom, liquid is collected to the top and bottom as shown in Fig. 3(a). On the other hand, when the tube is arranged as diverging parts are top and bottom, liquid is collected to the right and left sides as shown in Fig. 3(b). Effects of the tube arrangement have been reported elsewhere [6].

Table 1
Specification of test tubes

Test tube	S-1	G-1	H-1	H-2	H-3
d_o [mm]	7.00	7.00	7.00	7.00	7.00
d_i [mm]	6.40	6.36	6.40	6.34	6.38
p [mm]	–	0.41	0.35	0.35	0.33
l [mm]	–	0.21	0.22	0.18	0.17
b [mm]	–	0.20	0.23	0.15	0.18
t [mm]	–	0.07	0.05	0.09	0.09
α [deg]	–	41	18	33	20
β [deg]	–	18	16	14	8
k [mm]	–	0.25	0.25	0.27	0.27
number of fins	–	50	58	59	62
area ratio	1.00	1.81	2.15	1.83	1.93

The quasi-local condensation heat transfer coefficient of the each subsection is defined as follows.

$$\alpha = \frac{q}{T_s - T_{wi}} \tag{1}$$

Where, q is the heat flux obtained from the heat transfer rate Q and length Δz of each subsection, and the average inner diameter d_i, as follows:

$$q = \frac{Q}{\pi d_i \Delta z} \tag{2}$$

$$d_i = d_o - 2\left[k + \frac{l(p + t - b)}{2p}\right] \tag{3}$$

The average diameter d_i is an equivalent smooth tube diameter of which cross-section is equal to that of the micro-fin tube. The heat flux is defined with Eq. (2), because the mean inner diameter can be consistently employed for calculations of cross-sectional flow area, mass velocity, etc. T_s is the saturation temperature calculated from the measured pressure and heat transfer rate by assuming thermodynamic equilibrium in tube cross-section. The representative inner

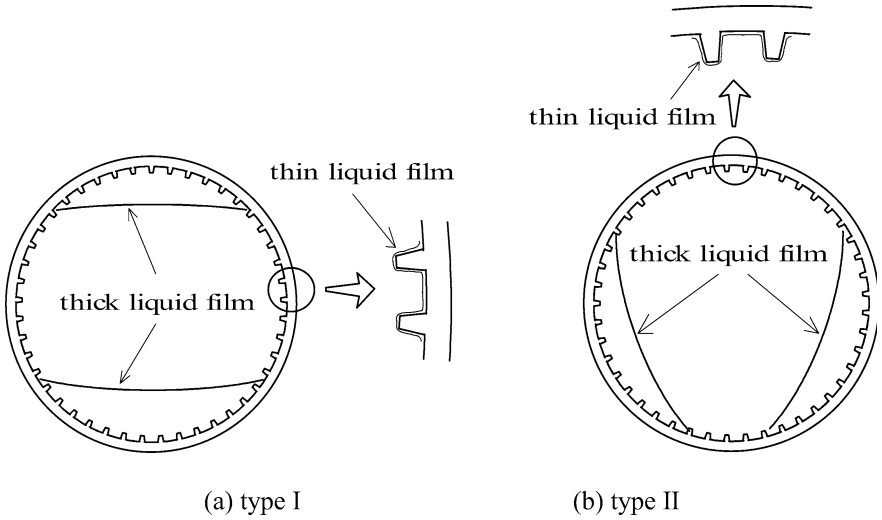

Fig. 3. Arrangements of herringbone tube: (a) Type I; (b) Type II.

wall temperature T_{wi} is calculated from the arithmetic mean of measured outer wall temperature T_{wo} and the heat transfer rate by using the following heat conduction equation.

$$T_{wi} = T_{wo} + Q\frac{\ln(d_o/d_i)}{2\pi\,\Delta z\lambda_w} \tag{4}$$

λ_w is the thermal conductivity of the copper tube. In the present experiment, the temperature difference between T_{wi} and T_{wo} was less than 0.03 K. Uncertainty of the heat transfer coefficient is estimated $\pm 10 \sim 40\%$.

Experiments were carried out under the conditions of saturation temperature at test section inlet of $T_s = 40\,^{\circ}\mathrm{C}$, mass velocity of $G = 100$, 200, 300, and 400 $\mathrm{kg\cdot m^{-2}\cdot s^{-1}}$. The working fluid is R410A, which is a quasi-azeotropic refrigerant mixture and may be treated in the same manner as a pure refrigerant because mass transfer effects are very small.

Flow configurations at tube outlet are observed by using R123 with another experimental apparatus. The experimental conditions are mass velocity $G = 100$, 200, 300 $\mathrm{kg\cdot m^{-2}\cdot s^{-1}}$, pressure $p = 0.2$ MPa, and quality $x = 0.1$ to 0.9 by 0.1 interval. Because of the pressure limitation of the apparatus, R410A could not be used as a working fluid.

Thermodynamic and transport properties of refrigerant are obtained by NIST REFPROP Ver. 6 [7].

3. Experimental results and discussions

Fig. 4 shows measured heat transfer coefficients of the smooth tube S-1, the helical micro fin tube G-1 and the three types of the herringbone micro fin tubes H-$1 \sim 3$ for three mass velocity conditions, $G = 100$, 300 and 400 $\mathrm{kg\cdot m^{-2}\cdot s^{-1}}$. The abscissa is wetness $1 - x$, which correspond to the refrigerant flow direction. x is thermodynamic equilibrium quality. All the herringbone micro fin tubes are arranged as type-I, in which liquid is collected to tube top and bottom parts. For all the conditions of all the tubes, the heat transfer coefficient decreases along downstream, as typical in-tube condensation behavior. The heat transfer coefficient of the helical micro fin tube is about 2 to 3 times higher than that of the smooth tube and the effect of mass velocity is very small. In the case of the herringbone micro fin tubes, H-1, H-2, and H-3, the heat transfer coefficient strongly depends on the mass velocity. The heat transfer coefficients of all the herringbone tubes are higher for higher mass velocity. For $G = 300$ and 400 $\mathrm{kg\cdot m^{-2}\cdot s^{-1}}$, they are higher than those of the helical micro fin tube. However, for $G = 100$ $\mathrm{kg\cdot m^{-2}\cdot s^{-1}}$, they are slightly lower. Even at high mass velocity, the enhancement rate is low in the high wetness region, $1 - x > 0.6 \sim 0.7$ for $G = 300$ $\mathrm{kg\cdot m^{-2}\cdot s^{-1}}$ and $1 - x > 0.7 \sim 0.8$ for $G = 400$ $\mathrm{kg\cdot m^{-2}\cdot s^{-1}}$.

Effects of the fin height are compared with comparison between H-1 and H-2. The heat transfer coefficients of both the tubes show almost the same values for all the mass velocity conditions. Because the fin apex angle α is smaller for the higher fin tube H-1 and the fin space b is bigger for H-1, which would work to enhance the heat transfer, effects of fin height may be ignored. This result is different from Kasai et al. [8] ones. They reported that higher heat transfer was obtained for the larger fin height. This difference may be caused by different experimental conditions. Fin heights of herringbone micro fin tube they used are 0.15 mm and 0.18 mm and the present ones are 0.18 mm and 0.22 mm. Therefore, it may be concluded that the effect of fin height is small if it is larger than 0.18 mm.

Effects of helix angle can be seen with the results of H-2 and H-3. In the low mass velocity condition, $G = 100$ $\mathrm{kg\cdot m^{-2}\cdot s^{-1}}$, both the tubes show almost the same heat transfer coefficient again. However, at high mass velocity condition the heat transfer coefficient of H-3, which has smaller helix angle, is lower than that of H-2, which has larger helix angle, while it is still higher than that of the helical micro fin tube G-1. The difference between H-2 and

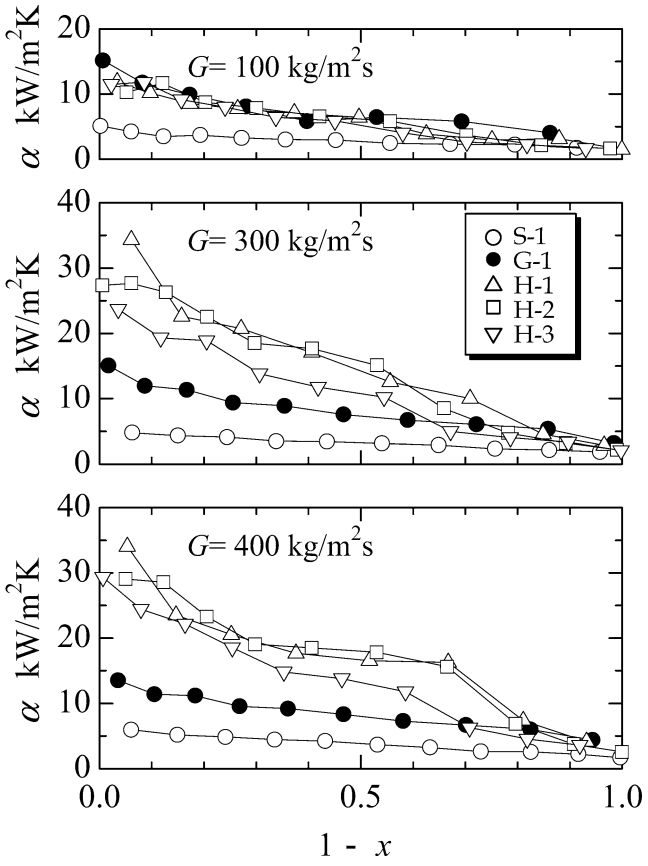

Fig. 4. Heat transfer coefficients of smooth, helical micro fin, and three types of the herringbone micro fin tubes for different mass velocity.

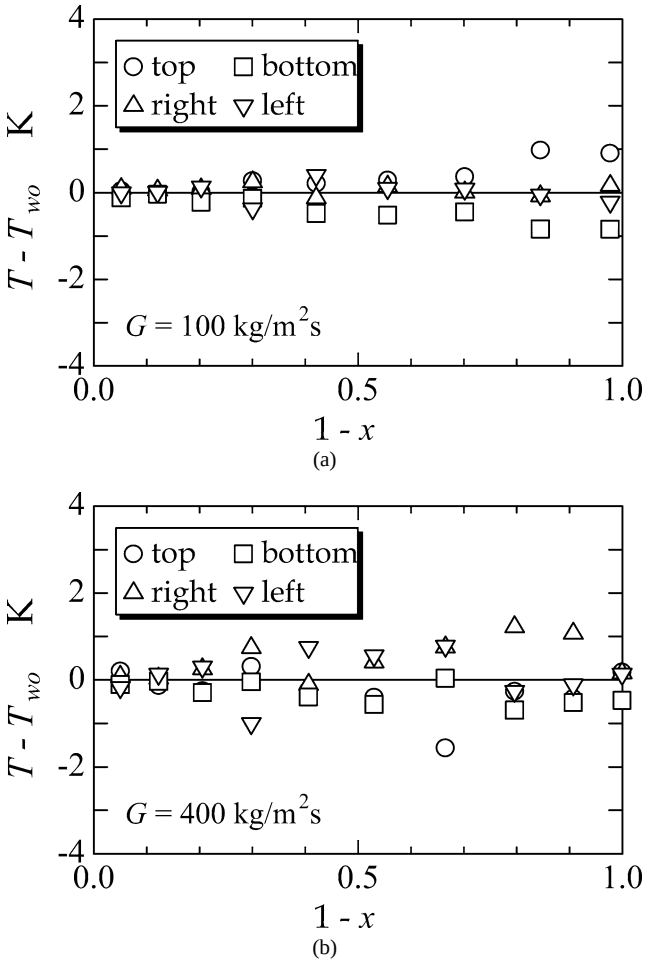

Fig. 5. Axial variations of the circumferential temperature distributions on the outer surface: (a) $G = 100\ \mathrm{kg{\cdot}m^{-2}{\cdot}s^{-1}}$; (b) $G = 400\ \mathrm{kg{\cdot}m^{-2}{\cdot}s^{-1}}$.

H-3 is somewhat larger for $G = 300\ \mathrm{kg{\cdot}m^{-2}{\cdot}s^{-1}}$ than for $G = 400\ \mathrm{kg{\cdot}m^{-2}{\cdot}s^{-1}}$. This result indicates that the liquid removal force is stronger for lager helix angle and the liquid film at the fin diverging part is thinner and its area is larger.

Because the heat transfer is enhanced by removing and collecting liquid, the heat transfer coefficient varies circumferentially, with higher heat transfer coefficient at fin diverging part and lower at fin converging part. The circumferential variation of the heat transfer coefficient, however, cannot be determined in the present experiment, since circumferential variation of heat flux cannot be measured. The circumferential temperature distribution may give good information for insight into situations of the circumferential heat transfer distribution. The wall temperature at a position where the heat transfer coefficient is the highest is presumably the highest. Fig. 5(a) and (b) show axial variation of the circumferential temperature distributions on the outer surface of the herringbone micro fin tube H-2 for mass velocities of $G = 100$ and $400\ \mathrm{kg{\cdot}m^{-2}{\cdot}s^{-1}}$, where the temperature difference between the mean value T_{wo} and the local values T at tube top, bottom, right and left sides are indicated. In the case of $G = 400\ \mathrm{kg{\cdot}m^{-2}{\cdot}s^{-1}}$ the temperatures of right and left sides are higher than those of top and bottom in most of the condensing region, although the data are fairly scattered. For $G = 100\ \mathrm{kg{\cdot}m^{-2}{\cdot}s^{-1}}$, however, the temperature at tube top is the highest, although temperatures at both sides tend to be higher at some point. These facts suggest that the liquid removal by the herringbone fins is not sufficiently available at low mass velocity condition.

In order to prove the effect of the herringbone fins on the liquid removal and collection, the flow configuration is observed at tube outlet by using another experimental apparatus. Because of pressure limit of the apparatus, R123 at 0.2 MPa is used as a working fluid instead of R410A. Fig. 6 shows typical photographs of H-1 for low and high mass velocity conditions, $G = 100$ and $300\ \mathrm{kg{\cdot}m^{-2}{\cdot}s^{-1}}$, at same quality, $x = 0.3$. At low mass velocity, tube bottom is covered with thick liquid film and the liquid flows out only from the tube bottom part. On the other hand, at high mass velocity, the liquid flows out from the bottom and top of the tube. From this observation, it may be concluded that the liquid removal and collection by the herringbone micro fins is effective in the high mass velocity region and ineffective in the low mass velocity region, which corresponds with the results obtained from the circumferential wall temperature distributions. Therefore, the heat transfer is enhanced only in the high mass velocity region, as shown in Fig. 4. Since only the qualitative flow observation is carried out and

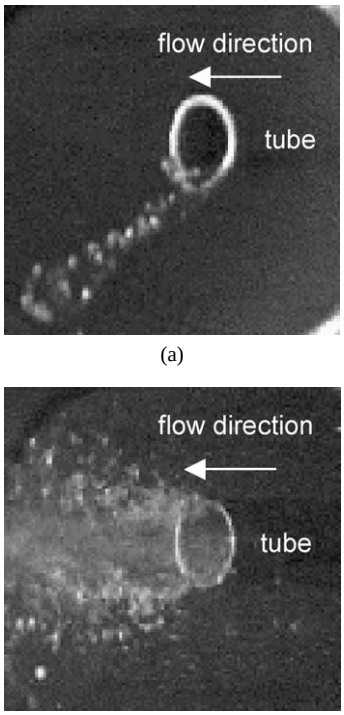

Fig. 6. Flow configuration at tube outlet of a herringbone micro fin tube: (a) $G = 100$ kg·m^{-2}·s^{-1} and $x = 0.3$; (b) $G = 300$ kg·m^{-2}·s^{-1} and $x = 0.3$.

the quantitative information cannot be measured, difference between three tube types, H-1, H-2 and H-3, is not observed.

Experimental conditions, in which flow configurations have been observed, are plotted on the modified Baker flow pattern map as shown in Fig. 7. The open symbols show the conditions where effect of herringbone fins is observed, which means that thick liquid films flow out from tube top and bottom like in Fig. 3(a) and in Fig. 6(b). On the other hand, closed symbols show the conditions where the herringbone fin effects are hardly observed like in Fig. 6(a). Although Fig. 7 is obtained from observed results of H-1, the flow configuration of H-2 and H-3 is similar to that of H-1. Lines of state variation during condensation of R410A for mass velocities $G = 100$, 300 and 400 kg·m^{-2}·s^{-1} are also plotted in the modified Baker flow pattern map.

The modified Baker flow pattern map is theoretically applicable to all kinds of fluid. The parameters λ and ψ in the flow pattern map are defined by the following equations.

$$\lambda = \left[\left(\frac{\rho_V}{\rho_A}\right)\left(\frac{\rho_L}{\rho_W}\right)\right]^{1/2} \tag{5}$$

$$\psi = \frac{\sigma_W}{\sigma}\left[\left(\frac{\mu_L}{\mu_W}\right)\left(\frac{\rho_W}{\rho_L}\right)^2\right]^{1/3} \tag{6}$$

Where the subscripts A and W refer to the physical properties of air and water at 1 atm and 20 °C, respectively.

Complete collection of liquid to tube top and bottom is observed in the high vapor velocity region, where vapor quality criteria are lower for higher mass velocity, such

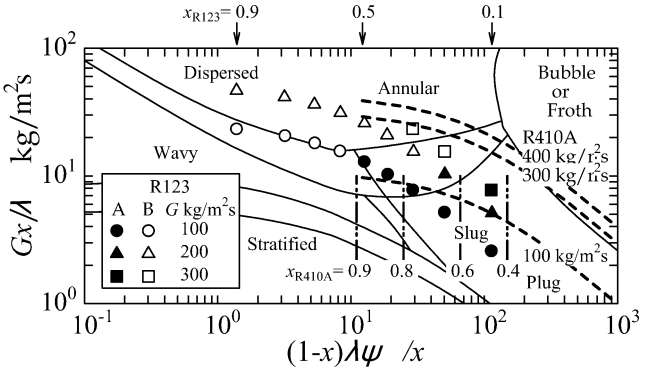

Fig. 7. Flow regime on the modified Baker flow pattern map.

as $x \geqslant 0.6$ for $G = 100$ kg·m^{-2}·s^{-1}, $x \geqslant 0.3$ for $G = 200$ kg·m^{-2}·s^{-1}, and $x \geqslant 0.2$ for $G = 300$ kg·m^{-2}·s^{-1}.

Although the modified Baker flow pattern map is for smooth tube, it may be considered that if flow conditions fall on the same place in the flow pattern map, the flow configuration of R410A is similar to the one of R123. As shown in Fig. 7, the variation of the state during condensation for $G = 100$ kg·m^{-2}·s^{-1} of R410A is on the region in which herringbone effect is not observed by flow configuration observation of R123. Therefore, it may be concluded that this is the reason why the heat transfer enhancements of all types of herringbone tubes at this mass flow rate are low, even slightly lower than those of the helical micro fin tube, and show the same values under the low mass velocity condition $G = 100$ kg·m^{-2}·s^{-1}. On the other hand, most part of the line $G = 400$ kg·m^{-2}·s^{-1} for R410A exists on the region of complete liquid removal and collection. These facts are the reason why a high heat transfer enhancement is obtained, as shown in Fig. 4. The following facts are also interesting. Steep decreases of the heat transfer coefficient of $G = 400$ kg·m^{-2}·s^{-1} appear at about $1 - x = 0.7$ for H-1 and H-2, and these qualities seem to be criteria of the liquid removal available region, obtained from the flow configuration, as shown in Fig. 7.

Fig. 8 shows the comparison of pressure drop between the smooth tube S-1, the helical micro fin tube G-1, and the three types of the herringbone micro fin tubes H-1 $\sim$ 3 under the three mass velocity conditions $G = 100$, 300 and 400 kg·m^{-2}·s^{-1}. It is indicated as the pressure differences between the test tube inlet P_0 and the local position P, $\Delta P = P - P_0$. The data of the smooth tube for $G = 100$ kg·m^{-2}·s^{-1} are not plotted because reliable data have not been obtained. In the case of $G = 100$ kg·m^{-2}·s^{-1} the pressure drops of all the tubes is small and the difference of each tube is hardly observed. On the other hand, in the case of $G = 300$ and 400 kg·m^{-2}·s^{-1} the difference of each tube clearly appears. Pressure drops of H-1 and H-2 are higher than those of G-1, which agrees with previous studies by Okazaki et al. [1], Ebisu et al. [2], Miyara et al. [3]. On the other hand, pressure drops of H-3, which has small helix angle, are lower than those of G-1. Because the heat transfer coefficient of H-3 is higher than that of G-

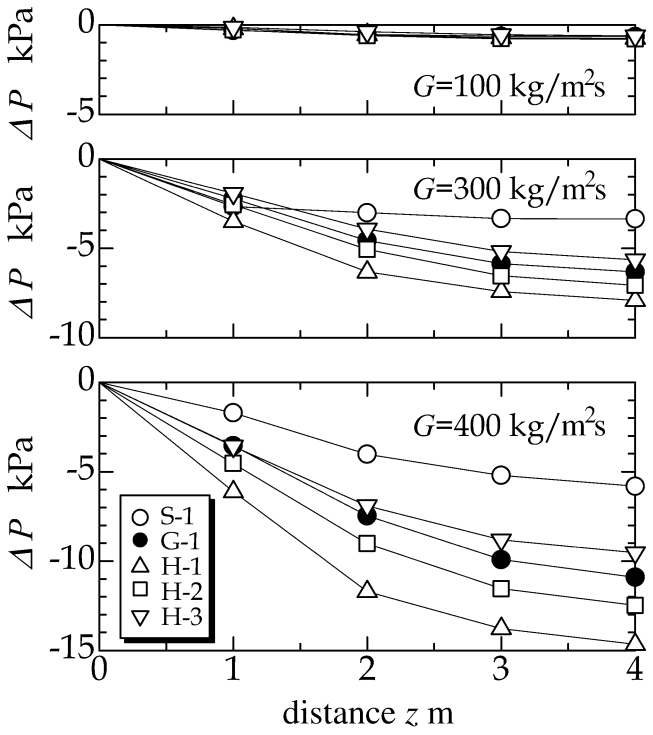

Fig. 8. Pressure drops of smooth, helical micro fin, and three types of the herringbone micro fin tubes for different mass velocity.

1 as shown in Fig. 4, this is a desirable result. From the comparison between H-1 and H-2, it is concluded that higher fin height leads higher-pressure drop. Since the heat transfer coefficient of H-1 and H-2 is almost the same, a higher fin is not necessary for improved performance.

4. Conclusion

Condensation heat transfer and pressure drop of R410A inside a smooth tube, a helical micro fin tube, and three types of herringbone micro fin tubes have been measured and flow configurations of R123 have been observed. From these results, following conclusions are obtained.

(1) The heat transfer coefficients of all types of the herringbone micro fin tubes are higher than those of the helical micro fin tube under high mass velocity condition, while they are slightly lower under low mass velocity condition.
(2) Effects of fin height on the heat transfer are small in the present experimental condition, while pressure drop is larger for higher fin.
(3) Although the heat transfer coefficient and pressure drop are lower for smaller helix angle, a herringbone micro fin tube which has higher heat transfer coefficient and lower pressure drop than those of a helical micro fin tube exists.
(4) Liquid removal by the herringbone micro fins is effective only under high vapor velocity condition.
(5) The low mass velocity condition of R410A in which the heat transfer enhancement is small corresponds to the region in which effects of the herringbone fins on liquid flow of R123 are hardly observed.

Acknowledgement

This study is supported by Matsushita Refrigeration Cooperation. Thanks are due to Mr. T. Mizuta, Mr. S. Otsuka, and Mr. T. Yamamoto for help with the experiments.

References

[1] T. Okazaki, Y. Sumida, Y. Tanimura, Evaporation heat transfer characteristics of alternative refrigerant R407C and R410A in a horizontal tube, in: Proc. 1996 JAR Annual Conference, 1996, pp. 49–52 (in Japanese).
[2] T. Ebisu, H. Fujino, K. Torikoshi, Heat transfer characteristics and heat exchanger performances for R407C using herringbone heat transfer tube, in: Proc. 1998 Internat. Refrig. Conf. at Purdue, 1998, pp. 343–348.
[3] A. Miyara, K. Nonaka, M. Taniguchi, Condensation heat transfer and flow pattern inside a herringbone-type micro-fin tube, Internat. J. Refrig. 23 (2000) 141–152.
[4] M.L. Chamra, R.L. Webb, M.R. Randlett, Advanced micro-fin tubes for condensation, Internat. J. Heat Mass Transfer 39 (1996) 1839–1846.
[5] M. Uchida, M. Itoh, N. Sikazono, T. Hatada, M. Kudoh, T. Otani, Using a cross-grooved inner surface for enhancement of heat transfer characteristics inside horizontal tubes for zeotropic refrigerant—first report: Condensation test, Trans. JSRAE 16 (1999) 189–194 (in Japanese).
[6] A. Miyara, Y. Otsubo, K. Takei, M. Taniguchi, Effect of fin direction on condensation heat transfer and flow pattern in a herringbone micro fin tube, in: Proc. 4th JSME–KSME Thermal Engrg. Conf., Vol. 3, 2000, pp. 781–786.
[7] M.O. McLinden, S.A. Klein, E.W. Lemmon, A.P. Peskin, NIST thermodynamic and transport properties of refrigerants and refrigerant mixtures—REFPROP, Version 6.01, 1998.
[8] K. Kasai, H. Fujino, T. Ebisu, K. Torikoshi, Heat transfer enhancement for alternative refrigerant using inductively welded heat transfer tube, in: Proc. 36th National Heat Transfer Symposium of Japan, Vol. 1, 1999, pp. 141–142 (in Japanese).